Received: 2 March 2019 | Revised: 6 July 2019 | Accepted: 9 July 2019

DOI: 10.1002/ardp.201900063

DPhG ARCH PHARM
Archiv der Pharmazie

FULL PAPER

Design, synthesis, and molecular docking studies of novel pyrazolyl 2-aminopyrimidine derivatives as HSP90 inhibitors

Akhila Mettu[1] | Venu Talla[2] | Deepti Madanlal Bajaj[2] | Naikal James Prameela Subhashini[3]

[1]Department of Pharmaceutical Chemistry, Gokaraju Rangaraju College of Pharmacy, Kukatpally, Hyderabad, India

[2]Department of Pharmacology, National Institute of Pharmaceutical Education and Research, Balanagar, Hyderabad, India

[3]Department of Chemistry, University College of Science, Osmania University, Hyderabad, India

Correspondence
Subhashini Naikal James Prameela, Department of Science, University College of Science, Osmania University, Hyderabad 500007, India.
Email: njsubhashini@yahoo.co.in

Funding information
Science and Engineering Research Board, Department of Science and Technology, Grant/Award Number: SR/WOSA/CS-1003/2014

Abstract

A series of novel pyrazolyl 2-aminopyrimidine derivatives (**7a**–**t**) were designed based on scaffold hopping techniques, synthesized and biologically evaluated for their HSP90 inhibition and anticancer activity. Several compounds exhibited potent HSP90 inhibition with IC_{50} values less than that of the reference standard 17-AAG (1.25 μM). The most potent compound **7t** displayed excellent HSP90 inhibition with an IC_{50} of 20 nM and in vitro antiproliferative potential against three cancer cell lines (IC_{50} < 5 μM). **7t** also induced dose dependent degradation of client proteins (pHER2 and pERK1/2) in Western blot analysis. Several structural features of **7p**–**t** oriented the molecules to retain all the essential binding interactions with HSP90, as observed by rationalized docking studies. Therefore, the *para*-nitrophenyl ring on the central pyrazole ring along with the 2-amino group on the pyrimidine ring are the crucial features in the development of novel HSP90 inhibitors based on this scaffold for targeted anticancer therapy.

KEYWORDS
active site, cancer, client proteins, HSP90 inhibitors, pyrazolyl pyrimidines

1 | INTRODUCTION

Cancer is a disorder of multiple mechanisms, progressive with severity and challenging life at various stages. It involves an imbalance in cellular growth with alteration of various mechanisms involved, leading to suppression of p53 gene and thereby evading apoptosis.[1] Heat shock protein 90 (HSP90) is a multichaperone complex recognized as a potential target for cancer.[2] It is reported that the levels of HSP90 constitute 5–10% in a cancer cell compared to 1% in normal cell.[3] Geldanamycin (GA) and radicicol (RA) are the first identified HSP90 inhibitors with limitations in their pharmacokinetic parameters. 17-*N*-Allyl amino-17-demethoxygeldanamycin (17-AAG), 17-dimethylaminoethylamino-17-demethoxygeldanamycin (17-DMAG) are the semisynthetic analogs of GA with lesser toxicity, however the side effects overlay their clinical use.[4,5] Later, various small molecules with diverse structures were proposed as N-terminal ATP competitive antagonists possessing purine (PU3), pyrazole (CCT018159, G3130), oxazole (AUY922), triazole (STA-9090), indazole (SNX2112, SNX5422), 2-aminopyrimidine (SNX6833, BIIB021, NVPHSP990) rings and most of them are still in clinical trials.[6–11] X-ray crystallographic studies and molecular docking studies of various reported inhibitors with HSP90 have shown hydrogen bonding with Asp93, Thr184, Asp54, Asn51, Lys58 amino acids, thereby proving their binding region as N-terminal ATP binding site.[12] Mostly, HER2 driven breast cancer and MAPK driven melanomas are most sensitive to HSP90 inhibitors.[13–15] Although the research on HSP90 inhibitors initiated decades back, still there exists a crave for new entities, due to pivotal role of HSP90 in cancer.

Many purine analogs were exploited as HSP90 inhibitors and several of them are in clinical trials (Figure 1). The SAR studies of these analogs have depicted the 2-aminopyrimidine scaffold as an essential moiety for activity.[16,17] Therefore, we have retained the same in our study. Further construction of our basic disubstituted pyrazolyl pyrimidine was based on BIIB021, a purine based conventional

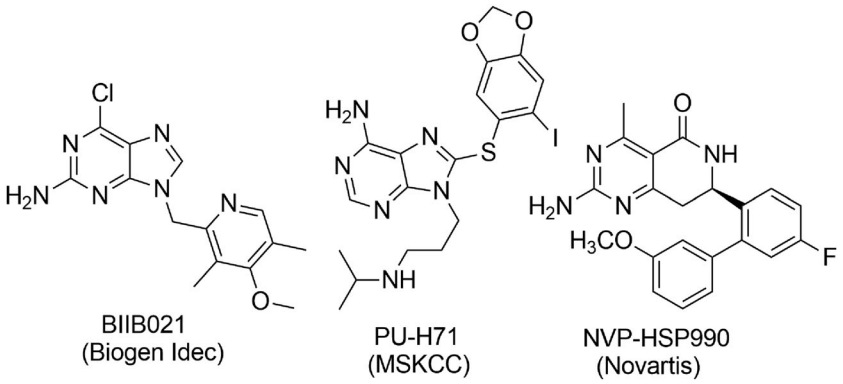

FIGURE 1 Aminopyrimidine based potent HSP90 inhibitors

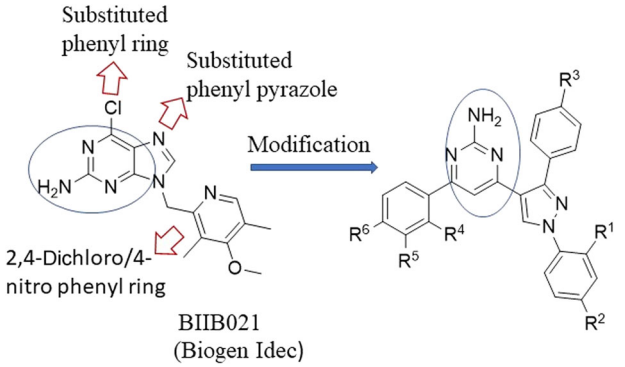

FIGURE 2 Design of the novel pyrazolyl pyrimidine derivatives **7a–t**

HSP90 inhibitor. As depicted in Figure 2, the substituted phenyl ring is supposed to occupy the chloro position of BIIB021, substituted phenyl pyrazole is presumed to be pyrazolo part of purine ring and 2,4-dichloro/4-nitro phenyl ring is theorized to replace 2,4-dichloro pyridine ring. A series of novel compounds with the proposed scaffold (**7a–t**) bearing various substituents were synthesized and evaluated for anticancer activity and HSP90 inhibition.

2 | RESULTS AND DISCUSSION

2.1 | Chemistry

Scheme 1 depicts the synthesis of disubstituted pyrazolyl pyrimidin-2-amines (**7a–t**). First step involved condensation of commercially available substituted phenyl hydrazine (**1a–c**) with substituted acetophenone (**2a,b**) to form hydrazones **3a–d**. The obtained product upon double Vilsmeier Haack reaction in the presence of two moles of phosphorous oxychloride and DMF yielded 1,3-disubstituted phenyl pyrazole-4-carbaldehydes **4a–d**.[18] The free aldehyde group when treated with substituted acetophenone (**5**) in the presence of strong base under reflux conditions yielded chalcones **6a–t**.[19] The chalcone moiety was then treated with guanidine hydrochloride using potassium

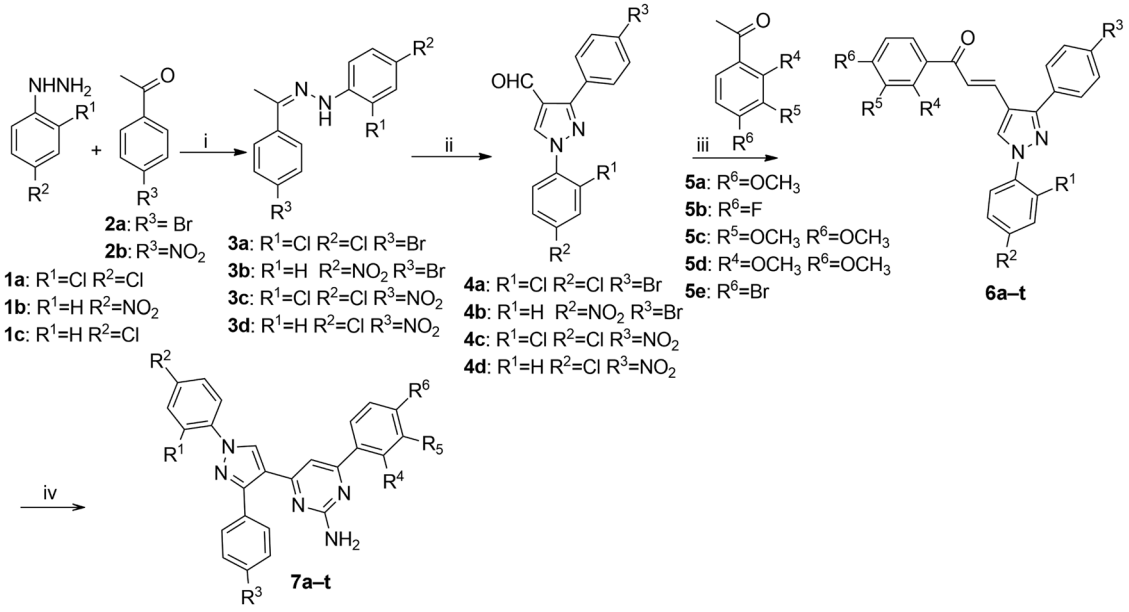

SCHEME 1 Synthesis of disubstituted pyrazolyl pyrimidin-2-amines **7a–t**. Reagents and conditions: (i) gla. AcOH (cat), methanol, 60–70°C, 6–7 hr, 80–90%. (ii) DMF/$POCl_3$, 80–90°C, 9–10 hr, 70–75%. (iii) 50% KOH, methanol, reflux, 12–16 hr, 40–55%. (iv) Guanidine-HCl, potassium *tert*-butoxide, DMF, reflux, 10–12 hr, 70–80%

TABLE 1 Structural details of synthesized compounds with results of the MTT and FP assay

							MTT assay (IC_{50} ± SD[a] in μM)			
#	R^1	R^2	R^3	R^4	R^5	R^6	MCF-7	MDA-MB-231	HCT116	FP assay (IC_{50} ± SD[a] in μM)
7a	Cl	Cl	Br	H	H	OCH_3	2.8 ± 0.3	1.6 ± 0.1	4.7 ± 0.3	4.08 ± 1.2
7b	Cl	Cl	Br	H	H	F	5.0 ± 1.8	4.4 ± 0.8	4.6 ± 0.2	6.63 ± 1.3
7c	Cl	Cl	Br	H	OCH_3	OCH_3	6.6 ± 0.7	3.5 ± 0.8	5.4 ± 0.1	3.08 ± 1.0
7d	Cl	Cl	Br	OCH_3	H	OCH_3	> 20	> 20	> 20	n/a
7e	Cl	Cl	Br	H	H	Br	> 20	> 20	> 20	n/a
7f	H	NO_2	Br	H	H	OCH_3	8.9 ± 1.9	3.6 ± 0.8	4.9 ± 0.1	n/a
7g	H	NO_2	Br	H	H	F	2.5 ± 0.2	5.4 ± 0.6	6.2 ± 0.3	2.04 ± 0.7
7h	H	NO_2	Br	H	OCH_3	OCH_3	1.7 ± 0.5	4.2 ± 0.7	4.4 ± 0.1	0.54 ± 0.05
7i	H	NO_2	Br	OCH_3	H	OCH_3	3.7 ± 0.8	2.9 ± 0.7	8.9 ± 1.0	n/a
7j	H	NO_2	Br	H	H	Br	1.7 ± 0.5	7.6 ± 0.9	> 20	0.85 ± 0.04
7k	Cl	Cl	NO_2	H	H	OCH_3	> 20	> 20	> 20	n/a
7l	Cl	Cl	NO_2	H	H	F	> 20	> 20	> 20	n/a
7m	Cl	Cl	NO_2	H	OCH_3	OCH_3	7.7 ± 3.2	16.4 ± 1	> 20	5.42 ± 1.24
7n	Cl	Cl	NO_2	OCH_3	H	OCH_3	> 20	> 20	15.5 ± 1.7	n/a
7o	Cl	Cl	NO_2	H	H	Br	9.6 ± 0.8	5.2 ± 2	> 20	8.54 ± 1.62
7p	H	Cl	NO_2	H	H	OCH_3	> 20	1.9 ± 0.8	6.0 ± 0.2	1.08 ± 0.08
7q	H	Cl	NO_2	H	H	F	3.8 ± 0.1	0.7 ± 0.6	4.3 ± 0.08	0.08 ± 0.004
7r	H	Cl	NO_2	H	OCH_3	OCH_3	> 20	0.8 ± 0.3	8.5 ± 0.7	1.06 ± 0.02
7s	H	Cl	NO_2	OCH_3	H	OCH_3	5.0 ± 0.5	2 ± 0.4	4.5 ± 0.5	0.05 ± 0.006
7t	H	Cl	NO_2	H	H	Br	2.4 ± 0.1	0.8 ± 0.4	4.8 ± 0.5	0.02 ± 0.003
17-AAG							0.25 ± 0.4	2 ± 0.5	0.2 ± 0.08	1.26 ± 0.03

Abbreviations: FP, flourescence polarization; MTT, 3-(4,5-dimethylthiazol-2-yl)-2,5-diphenyltetrazolium bromide; SD, standard deviation.
[a]All results are mean of at least three independent determinations performed in duplicate. n/a, not available.

tertiary butoxide as base to furnish the final compounds **7a–t**. All the synthesized compounds were purified by column chromatography using ethyl acetate/petroleum ether solvent system.

The synthesized compounds **7a–t** were structurally confirmed by IR, ^{1}H-NMR, ^{13}C-NMR, ESI-MS techniques. In general, the IR spectrum of all the compounds exhibited characteristic peaks of free amino group (NH_2) at 3,450–3,400 cm^{-1} and 1,630–1,580 cm^{-1} for aromatic rings (C=C). In the ^{1}H-NMR spectra, the methoxy groups of compounds **7a**, **7c**, **7d**, **7 f**, **7h**, **7i**, **7k**, **7m**, **7n**, **7p**, **7r** and **7s** appeared in the range of δ 3.95–3.50. The amino group of all the compounds was in the range of δ 5.85–5.10 and its protons were exchangeable with D_2O, all the aromatic protons were observed in the range of δ 8.80–6.84. The ^{13}C-NMR spectra represent the signal for methoxy carbons of compounds **7a**, **7c**, **7d**, **7f**, **7h**, **7i**, **7k**, **7m**, **7n**, **7p**, **7r**, and **7s** at δ 56.1–55.2, the aromatic carbons of all the compounds between δ 165–101 ppm. All the compounds were analyzed by ESI-MS analysis to give peaks $[M+H]^+$ or $[M+Na]^+$ corresponding to their molecular weights.

2.2 | HSP90 inhibition and antiproliferative assays

All the test compounds (**7a–t**) and the reference compound 17-AAG were evaluated for HSP90 inhibition by fluorescence polarization assay and in vitro antiproliferative activities by the 3-(4,5-dimethylthiazol-2-yl)-2,5-diphenyltetrazolium bromide (MTT) assay on two human breast carcinomas (MCF-7 and MDA-MB-231) and colon carcinoma (HCT116). The results are depicted in Table 1. Based on the substitutions of rings A and B on pyrazole, all the test compounds are grouped into four types (Figure 3). Type 4 (**7p–t**) with *para*-chloro group on ring A and *para*-nitro group on ring B were most active in both the assays performed with IC_{50} valves for MTT assay in the range of 2.4–20 μM, 0.7–2 μM and 4.3–8.5 μM on MCF-7, MDA-MB-231, and HCT-116 cell lines, respectively, and 0.02–1.08 μM in FP assay for HSP90 inhibition; type 2 (**7f–j**) with *para*-nitro group on ring A and *para*-bromo group on ring B have good anti-proliferative activities with IC_{50} valves in the range of 1.7–8.9 μM, 2.9–7.6 μM, 4.4–20 μM on MCF-7, MDA-MB-231, and HCT116 cell lines, respectively, with optimum HSP90 inhibition (IC_{50} at 0.85–2.04 μM); type 1 series (**7a**–e) with 2,4-dichloro substitution on ring A and *para*-bromo substitution on ring B have average to good antiproliferative activities with IC_{50} valves in the range of 2.8–20 μM, 1.6–20 μM, 4.6–20 μM on MCF-7, MDA-MB-231, and HCT116 cell lines, respectively, and exhibit moderate HSP90 inhibition (IC_{50} at 3.08–6.63 μM); type 3 (**7k–o**) with 2,4-dichloro substitution on ring A and *para*-nitro group on ring B were least active in both the tests performed with IC_{50} values in the range of 7.7–20 μM, 5.2–20 μM, 15.5–20 μM on MCF-7, MDA-MB-231, and HCT116 cell lines,

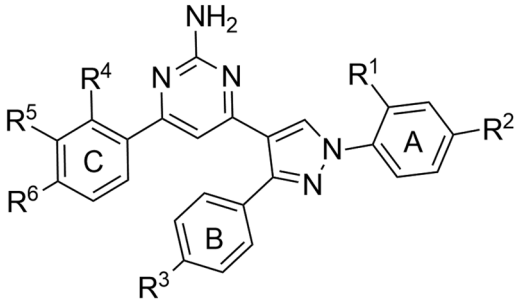

Type 1 series: **7a–e** (R^1=Cl, R^2=Cl, R^3=Br)
Type 2 series: **7f–j** (R^1=H, R^2=NO_2, R^3=Br)
Type 3 series: **7k–o** (R^1=Cl, R^2=Cl, R^3=NO_2)
Type 4 series: **7p–t** (R^1=H, R^2=Cl, R^3=NO_2)

FIGURE 3 Disubstituted pyrazolyl pyrimidin-2-amine scaffold illustrating the four variants of the compounds

respectively and exhibit moderate HSP90 inhibition (IC_{50} at 5.42–8.54 μM). Compounds **7q**, **7s**, and **7t** displayed significantly good results in all the three cell lines (MTT assay) with IC_{50} values ≤5 μM and potent HSP90 inhibition at 80, 50, and 20 nM, respectively, than standard 17-AAG (1.25 μM). Compound **7t** exhibited the highest HSP90 inhibition as well as potent in vitro antiproliferative efficacy against the three cancer cell lines (IC_{50} values of 2.4, 0.8, 4.8 for MCF-7, MDA-MB-231, HCT-116, respectively). Overall, mono-substitution on ring A with nitro group on ring B and amino group of pyrimidine are the essential features of this scaffold for HSP90 inhibition and therefore could be the reason for the higher activity profiles observed with type 4 series.

2.3 | Docking

All the synthesized compounds with 17-AAG were docked at N-terminal ATP binding site HSP90α using Glide program embedded in Maestro 9.1 on Schrodinger engine. 5LRZ was downloaded from Protein Data Bank due to the structural similarity of its ligand with our synthesized compounds and binding affinities were analyzed along with essential hydrogen bonding interactions with AsH93 (protonated form of Asp93), Thr184, Asn51, Asp54, Lys58.[20,21] Compounds **7f–j**, **7p–t** being monosubstituted on rings A and B oriented perfectly into the pockets of active site. The nitro group on phenyl ring B in **7p–t** established the crucial interaction with AsH93 and therefore could be the reason for the good binding affinities observed with this series. The pyrimidine ring occupies the center of active site with its free amino group orienting

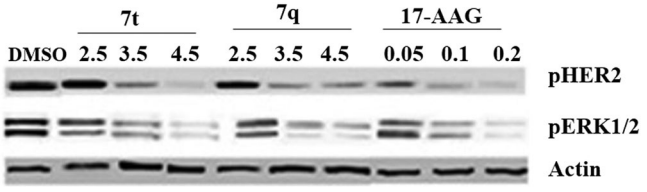

FIGURE 4 Effects of the test compounds on HSP90 client proteins in MCF-7 cells

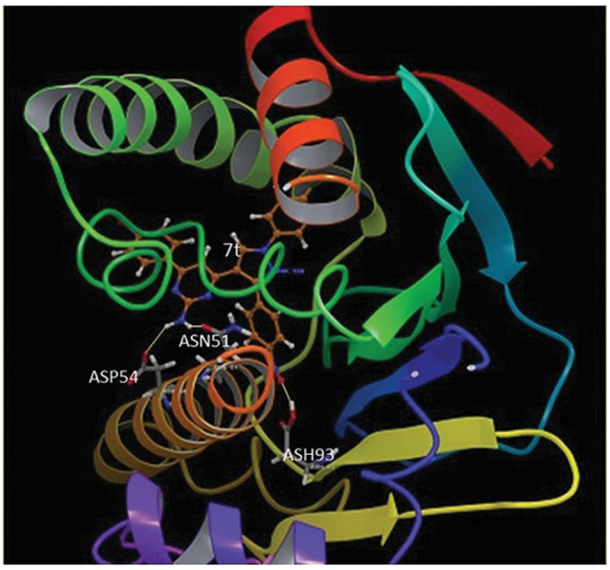

FIGURE 5 Receptor interactions of compound **7t** (orange) at the active site of HSP90. A yellow line represents hydrogen bonding with the respective amino acid

toward acidic hydrophilic pocket and hydrogen bonding with Asn51 and Asp54 as depicted in Figure 5 for compound **7t**. The substituents on the phenyl ring C occupies the basic pocket, hydrogen bonding methoxy group with Lys58. Surrounding these hydrophilic sites are the hydrophobic interactions with Ala55, Ile96, Met98, Leu107, Ile110, Ala111, Gly135, Phe138, Tyr139, Trp162, and Val186 amino acids (Figure 6). Although **7k–o** also possess *para*-nitro group on phenyl ring B, the presence of disubstitution on phenyl ring A oriented the compound in a different mode thereby hindering the key interaction with AsH93, which could be the reason for lesser activity profiles.

2.4 | Structure–activity relationship

Scaffold: Disubstituted pyrazolyl pyrimidin-2-amine pharmacophore was the crucial moiety of all compounds (**7a–t**). The amino group retained essential interactions with HSP90 protein and the

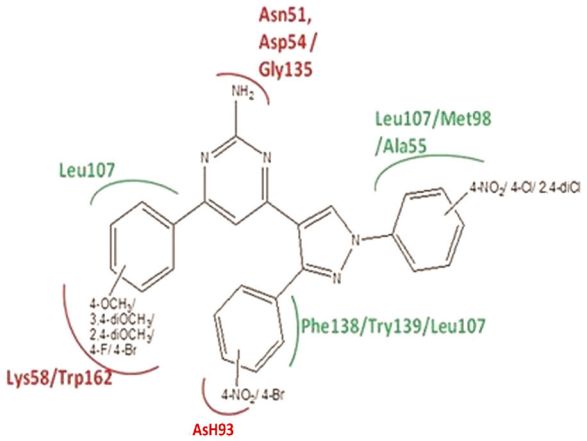

FIGURE 6 Receptor interactions of compounds **7a–t** at the active site of HSP90

disubstituted pyrazolyl pyrimidine scaffold oriented perfectly into the active site of protein as observed by docking studies.

Ring A: Compounds with mono-substitution at *para* position on ring A displayed good HSP90 inhibition (**7f–j**, **7p–t**) compared to disubstituted compounds (**7a–e**, **7k–o**). 4-Chloro substituted compounds (**7p–t**) were more active than 4-nitro substituted ones (**7f–j**). This could be due to the increased hydrophobic interactions seen with chloro over nitro group.

Ring B: Para-nitro substitution (**7a–j**) was more predominate than *para*-bromo as observed in compounds **7k–t**. Also, the nitro group retained the essential hydrogen bonding with protonated Asp93 in docking studies (Figure 6).

Ring C: Substituents on ring C (R^4–R^6) determined the various activity profiles of all the compounds. Halo substituted compounds (**7j**, **7q**, **7t**) were more active than methoxy substituted ones (**7h**, **7p**, **7r**, **7s**). The bromo substitution (**7t**, **7j**) was predominate than fluoro substitution (**7q**, **7g**). This could be due to increased hydrophobic interactions seen with bromo over fluoro counterpart. Dimethoxy substituted compounds (**7s**, **7r**, **7c**) were more active than monomethoxy substituted ones (**7p**, **7a**). No particular trend was observed with position of disubstitution.

2.5 | Western blot analysis

Effect of HSP90 inhibition was observed by the degradation of its client proteins. pHER2 expressing breast cancers and altered MAPK signaling induced cancers are the most prevalent ones and therefore were selected in our study. Two compounds (**7q**, **7t**) and reference compound 17-AAG were tested for their effect on the two client proteins (pHER2 and pERK1/2) on MCF-7 cell line. Figure 4 displays dose dependent degradation of pHER2 and pErk1/2 with increasing concentrations of compounds (2.5, 3.5, 4.5 μM). β-Actin was the loading control and 17-AAG was taken at 0.05, 0.1, and 0.2 μM concentrations.

3 | CONCLUSION

The present work has designed a novel scaffold with disubstituted pyrazolyl pyrimidin-2-amine moiety based on scaffold hopping and developed a series of compounds **7a–t** as novel anticancer agents with HSP90 inhibition. Among these, compound **7t** displayed excellent HSP90 inhibition at nanomolar scale (20 nM) and in vitro antiproliferative potential against three cancer cell lines (IC_{50} < 5 μM). HSP90 inhibition was also evidenced via inhibition of client proteins (pHER2 and pERK1/2) by compounds **7t** and **7q**. Molecular docking studies well appreciated compounds **7p–t** as excellent HSP90 inhibitors. The presence of mono substitution at *para* position on rings A and B of pyrazole especially with *p*-nitro group on ring B and 2-amino group of pyrimidine are the pharmacophoric essentials of this series at active site of HSP90. Therefore, the higher potency of these drugs with targeted action make them superior over conventional HSP90 inhibitors.

4 | EXPERIMENTAL

4.1 | Chemistry

4.1.1 | General

All the melting points were determined using BÜCHI Melting Point B-450 apparatus (Büchi Labortechnik, Switzerland). IR spectra were recorded on Shimadzu IR Affinity-1, FT-IR spectrophotometer. Nuclear magnetic resonance (^1H and ^{13}C NMR) spectra were recorded with Avance 300 spectrophotometer with chemical shifts in parts per million (ppm, δ) downfield from TMS as an internal standard using $CDCl_3$ or DMSO solvent. High resolution mass spectra were recorded with Agilent QTOF mass spectrometer. Commercially available reagents and solvents were procured from Sigma Aldrich/Merck/TCI and used without any purification unless stated. All the synthesized compounds were purified on Buchi Flash Chromatography using Merck silica gel 200–400#.

The spectral data of the investigated compounds are provided as Supporting Information. Also, their InChI codes together with biological evaluation data are also provided as Supporting Information.

4.1.2 | Synthetic procedures of compounds 3a–d, 4a–d, 6a–t

Synthesis of substituted acetophenone phenyl hydrazones (**3a–d**) involves condensation of respective acetophenones **1a–c** with substituted phenyl hydrazine **2a/2b** and then synthesis of 1,3-di-(substituted)phenyl-1*H*-pyrazole-4-carboxaldehyde (**4a–d**) using the Vilsmeier-Haack reagent ($POCl_3$/DMF); employing a similar procedure followed by Kira et al.[18] Their analytical and spectroscopic data agreed with reported literature. Pyrazolyl chalcones (**6a–t**) were synthesized by Claisen-Schmidt condensation of intermediates **4a–d** (0.01 mol) with appropriate aldehydes **5a–e** (0.01 mol) in methanol (30 ml) and refluxed in the presence of base (40% potassium hydroxide) for 12–14 hr. The reaction mixture was then poured into crushed ice followed by neutralization with HCl. The solid separated was filtered, dried and crystallized from ethanol. The purity of the chalcones was checked by TLC. The IR spectra showed typical absorption bands at 1,660–1,627, 1,518–1,605, 1,332–1,507 cm^{-1} corresponding to C=O, C=C, and NO_2 functionalities, respectively. In the ^1H-NMR spectra, doublet at 7.67–7.87 and 7.60–7.69 ppm represents C=C bond formation as reported by Insuasty et al.[19]

4.1.3 | General synthetic procedure for disubstituted pyrazolyl pyrimidin-2-amines (7a–t)

To the solution of intermediates **6a–t** (10 mmol) in DMF (10 ml), guanidine hydrochloride (10 mmol) was added followed by potassium *tert*-butoxide (1 mmol) and refluxed for 6–8 hr. Then, the reaction mixture was quenched with dil. HCl and extracted into ethyl acetate (50 ml × 3). The organic layer was collected and the obtained crude solid was purified by column chromatography (EtOAc/Hex = 1:2) to obtain compounds **7a–t**.

4-(3-(4-Bromophenyl)-1-(2,4-dichlorophenyl)-1H-pyrazol-4-yl)-6-(4-methoxyphenyl)pyrimidin-2-amine (**7a**)

Yield 65%; m.p. 145°C; FT-IR (KBr) ν/cm^{-1}: 3,437 (NH_2), 2,748 (CH aliphatic), 1,600 (C=C aromatic). ^{1}H-NMR (300 MHz, $CHCl_3$) δ (ppm): 3.85 (s, 3H, OCH_3), 5.20 (s, 2H, NH_2) (D_2O exchangeable), 6.84–6.99 (m, 4H, ArH), 7.39–7.42 (d, 1H, ArH, *J* = 9), 7.57–7.66 (m, 5H, ArH), 7.74–7.77 (d, 2H, ArH, *J* = 9), 8.41 (s, 1H, ArH). ^{13}C-NMR (75 MHz, $CDCl_3$): δ 164.8, 163.6, 160.0, 159.7, 147.8, 143.7, 134.5, 133.3, 132.6, 132.5, 131.8, 131.6, 128.7, 128.3, 128.1, 125.5, 123.1, 122.7, 117.8, 104.5, 111.3, 55.8. ESI-MS: *m/z* 567 ($M+H^+$).

4-(3-(4-Bromophenyl)-1-(2,4-dichlorophenyl)-1H-pyrazol-4-yl)-6-(4-fluorophenyl)pyrimidin-2-amine (**7b**)

Yield 70%; m.p. 220°C; FT-IR (KBr) ν/cm^{-1}: 3,433 (NH_2), 1,629 (C=C aromatic), 1,226 (C–F). ^{1}H-NMR (300 MHz, $CHCl_3$) δ (ppm): 5.15 (s, 2H, NH_2) (D_2O exchangeable), 6.88 (s, 1H, ArH), 7.11–7.14 (d, 2H, ArH, *J* = 9), 7.38–7.42 (dd, 1H, ArH, *J* = 6), 7.57–7.59 (m, 5H, ArH), 7.63 (s, 1H, ArH), 7.77–7.82 (q, 2H, ArH), 8.43 (s, 1H, ArH). ^{13}C-NMR (75 MHz, $CDCl_3$): 164.8, 163.2, 158.9, 149.7, 145.6, 136.9, 135.6, 132.3, 132.1, 130.8, 130.2, 128.9, 128.4, 127.1, 123.0, 121.8, 115.9, 113.6, 105.5, 101.9, 101.3. ESI-MS: *m/z* 556 ($M+H^+$).

4-(3-(4-Bromophenyl)-1-(2,4-dichlorophenyl)-1H-pyrazol-4-yl)-6-(3,4-dimethoxyphenyl)pyrimidin-2-amine (**7c**)

Yield 70%; m.p. 160°C; FT-IR (KBr) ν/cm^{-1}: 3,437 (NH_2), 2,852 (CH aliphatic), 1,583 (C=C aromatic). ^{1}H-NMR (300 MHz, $CHCl_3$) δ (ppm): 3.91 (s, 3H, OCH_3), 3.92 (s, 3H, OCH_3), 5.10 (s, 2H, NH_2) (D_2O exchangeable), 6.88 (s, 1H, ArH), 6.91 (s, 1H, ArH), 7.32–7.34 (d, 1H, ArH, *J* = 6.4), 7.37–7.42 (m, 2H, ArH), 7.59 (m, 5H, ArH), 7.63–7.66 (d, 1H, ArH, *J* = 9.2), 8.45 (s, 1H, ArH). ^{13}C-NMR (75 MHz, $CDCl_3$): 165.2, 163.4, 159.8, 151.2, 149.0, 147.5, 136.2, 134.8, 133.4, 131.6, 130.8, 130.5, 129.7, 128.9, 128.4, 128.1, 122.9, 120.8, 120.0, 110.9, 109.4, 105.2, 55.9. ESI-MS: *m/z* 598 ($M+H^+$).

4-(3-(4-Bromophenyl)-1-(2,4-dichlorophenyl)-1H-pyrazol-4-yl)-6-(2,4-dimethoxyphenyl)pyrimidin-2-amine (**7d**)

Yield 70%; m.p. 140°C; FT-IR (KBr) ν/cm^{-1}: 3,444 (NH_2), 2,752 (CH aliphatic), 1583 (C=C aromatic). ^{1}H-NMR (300 MHz, $CHCl_3$) δ (ppm): 3.85 (s, 3H, OCH_3), 3.92 (s, 3H, OCH_3), 5.25 (s, 2H, NH_2) (D_2O exchangeable), 6.85–6.87 (d, 1H, ArH), 6.90 (s, 1H, ArH), 7.38–7.39 (d, 1H, ArH, *J* = 3.1), 7.40–7.42 (d, 1H, ArH, *J* = 6.3), 7.44 (s, 1H, ArH), 7.56–7.57 (m, 2H, ArH), 7.63–7.66 (d, 2H, ArH, *J* = 9.5), 8.25–8.27 (m, 2H, ArH); 8.42 (s, 1H, ArH). ^{13}C-NMR (75 MHz, $CDCl_3$): 165.7, 163.3, 162.7, 160.6, 159.6, 146.9, 142.6, 134.7, 133.5, 133.6, 132.6, 131.8, 131.6, 131.2, 129.4, 127.6, 123.5, 122.4, 110.2, 107.5, 104.9, 101.8, 98.6, 56.2, 55.4. ESI-MS: *m/z* 619 ($M+Na^+$).

4-(4-Bromophenyl)-6-(3-(4-bromophenyl)-1-(2,4-dichlorophenyl)-1H-pyrazol-4-yl)pyrimidin-2-amine (**7e**)

Yield 45%; m.p. 230°C; FT-IR (KBr) ν/cm^{-1}: 3,448 (NH_2), 1,629 (C=C aromatic), 669 (C–Br). ^{1}H-NMR (300 MHz, $CHCl_3$) δ (ppm): 5.30 (s, 2H, NH_2) (D_2O exchangeable), 6.85 (s, 1H, ArH), 7.32–7.45 (dd, 2H, ArH), 7.55–7.71 (m, 7H, ArH), 7.84–7.97 (m, 2H, ArH), 8.46 (s, 1H, ArH). ^{13}C-NMR (75 MHz, $CDCl_3$): 165.1, 163.7, 162.5, 146.7, 142.3, 133.8, 132.8, 133.2, 132.7, 132.3, 131.5, 130.0, 128.7, 122.5, 123.6, 103.7, 101.7. ESI-MS: *m/z* 616 ($M+H^+$).

4-(3-(4-Bromophenyl)-1-(4-nitrophenyl)-1H-pyrazol-4-yl)-6-(4-methoxyphenyl)pyrimidin-2-amine (**7f**)

Yield 75%; m.p. 240°C; FT-IR (KBr) ν/cm^{-1}: 3,404 (NH_2), 2,723 (CH aliphatic), 1,550 (C=C aromatic), 1,334 (NO_2). ^{1}H-NMR (300 MHz, $CHCl_3$) δ (ppm): 3.76 (s, 3H, OCH_3), 5.69 (s, 2H, NH_2) (D_2O exchangeable), 6.83–6.86 (d, 2H, ArH, *J* = 9.3), 6.88 (d, 1H, ArH), 7.47–7.59 (m, 4H, ArH), 7.74–7.77 (d, 2H, ArH, *J* = 9.5), 8.03–8.06 (d, 2H, ArH, *J* = 9.2), 8.26–8.29 (d, 2H, ArH, *J* = 9.3), 8.83 (s, 1H, ArH). ^{13}C-NMR (75 MHz, $CDCl_3$): 165.2, 163.4, 161.8, 159.3, 145.8, 143.6, 131.7, 131.3, 130.6, 129.0, 128.4, 125.4, 124.3, 123.3, 118.7, 114.1, 105.1, 101.4, 55.8. ESI-MS: *m/z* 565 ($M+H^+$).

4-(3-(4-Bromophenyl)-1-(4-nitrophenyl)-1H-pyrazol-4-yl)-6-(4-fluorophenyl)pyrimidin-2-amine (**7g**)

Yield 75%; m.p. 240°C; FT-IR (KBr) ν/cm^{-1}: 3,404 (NH_2), 1,550 (C=C aromatic), 1338 (NO_2), 1,224 (C–F). ^{1}H-NMR (300 MHz, $CHCl_3$) δ (ppm): 5.80 (s, 2H, NH_2) (D_2O exchangeable), 6.93 (s, 1H, ArH), 7.02–7.07 (d, 2 H, ArH), 7.48–7.59 (m, 4H, ArH), 7.83 (d, 2H, ArH), 8.05–8.07 (d, 2H, ArH, *J* = 6.4), 8.27–8.30 (d, 2H, ArH, *J* = 9.4), 8.89 (s, 1H, ArH). ^{13}C-NMR (75 MHz, $CDCl_3$): 165.7, 164.8, 162.5, 162.0, 146.1, 145.4, 145.0, 132.4, 132.0, 131.8, 131.5, 130.5, 128.7, 123.5, 123.1, 118.9, 115.0, 103.9. ESI-MS: *m/z* 553 ($M+H^+$).

4-(3-(4-Bromophenyl)-1-(4-nitrophenyl)-1H-pyrazol-4-yl)-6-(3,4-dimethoxyphenyl)pyrimidin-2-amine (**7h**)

Yield 70%; m.p. 260°C; FT-IR (KBr) ν/cm^{-1}: 3,423 (NH_2), 2,746 (CH aliphatic), 1,629 (C=C aromatic), 1,332 (NO_2). ^{1}H-NMR (300 MHz, $CHCl_3$) δ (ppm): 3.80 (s, 3H, OCH_3), 3.82 (s, 3H, OCH_3), 5.62 (s, 2H, NH_2) (D_2O exchangeable), 6.82–6.84 (d, 2H, ArH), 7.29 (s, 1H, ArH), 7.37–7.40 (d, 1H, ArH, *J* = 9), 7.50–7.59 (m, 4H, ArH), 8.03–8.06 (d, 2H, ArH), 8.27–8.30 (d, 2 H, ArH, *J* = 9), 8.83 (s, 1H, ArH). ^{13}C-NMR (75 MHz, $CDCl_3$): 165.1, 162.6, 161.1, 153.1, 149.6, 146.7, 146.3, 145.7, 131.9, 131.5, 130.6, 127.8, 123.9, 123.3, 117.6, 115.9, 111.4, 107.8, 104.6, 101.1, 56.5. ESI-MS: *m/z* 595 ($M+H^+$).

4-(3-(4-Bromophenyl)-1-(4-nitrophenyl)-1H-pyrazol-4-yl)-6-(2,4-dimethoxyphenyl)pyrimidin-2-amine (**7i**)

Yield 78%; m.p. 200°C; FT-IR (KBr) ν/cm^{-1}: 3,446 (NH_2), 2,796 (CH aliphatic), 1,581 (C=C aromatic), 1,336 (NO_2). ^{1}H-NMR (300 MHz, $CHCl_3$) δ (ppm): 3.91 (s, 3H, OCH_3), 3.93 (s, 3H, OCH_3), 5.20 (s, 2H, NH_2) (D_2O exchangeable), 6.86–6.89 (d, 2H, ArH), 7.31 (s, 1H, ArH), 7.36–7.38 (d, 1H, ArH), 7.55–7.66 (m, 4H, ArH), 7.99–8.02 (d, 2H, ArH, *J* = 6.5), 8.36–8.39 (d, 2H, ArH, *J* = 9.0), 8.66 (s, 1H, ArH). ^{13}C-NMR (75 MHz, $CDCl_3$): 165.1, 163.7, 160.7, 159.8, 159.4, 147.6, 145.1, 143.6, 132.7, 132.2, 131.8, 129.5, 127.7, 123.5, 118.7, 109.6, 107.2, 103.7, 101.9, 98.6, 56.3, 55.4. ESI-MS: *m/z* 595 ($M+H^+$).

4-(4-Bromophenyl)-6-(3-(4-bromophenyl)-1-(4-nitrophenyl)-1H-pyrazol-4-yl)pyrimidin-2-amine (**7j**)

Yield 72%; m.p. 260°C; FT-IR (KBr) ν/cm^{-1}: 3,411 (NH_2), 1,579 (C=C aromatic), 1,334 (NO_2), 601 (C–Br). ^{1}H-NMR (300 MHz, $CHCl_3$) δ (ppm): 5.11 (s, 2H, NH_2) (D_2O exchangeable), 6.93 (d, 1H, ArH), 7.51–7.67 (m, 6H, ArH), 7.84–7.87 (d, 2H, ArH, *J* = 8.5), 8.00–8.03 (d, 2H, ArH, *J* = 9), 8.30–8.33 (d, 1H, ArH, *J* = 9.4), 8.38–8.41 (d, 1H, ArH, *J* = 9.2), 8.64 (s, 1H, ArH). ^{13}C-NMR (75 MHz, $CDCl_3$): 165.7, 163.3, 162.0, 145.8, 145.5, 143.2, 135.7, 132.6, 132.0, 131.9, 128.4, 124.6, 123.7, 119.4, 103.7, 101.3. ESI-MS: *m/z* 554 ($M+H^+$).

4-(1-(2,4-Dichlorophenyl)-3-(4-nitrophenyl)-1H-pyrazol-4-yl)-6-(4-methoxyphenyl)pyrimidin-2-amine (**7k**)

Yield 74%; m.p. 180°C; FT-IR (KBr) ν/cm^{-1}: 3,421 (NH_2), 2,794 (CH aliphatic), 1,631 (C=C aromatic), 1,344 (NO_2). ^{1}H-NMR (300 MHz, $CHCl_3$) δ (ppm): 3.85 (s, 3H, OCH_3), 5.07 (s, 2H, NH_2) (D_2O exchangeable), 6.92–6.95 (d, 3H, ArH), 7.41–7.44 (dd, 1 H, ArH, *J* = 6), 7.60–7.66 (dd, 2H, ArH), 7.81–7.84 (d, 2H, ArH, *J* = 9), 7.90–7.93 (d, 2H, ArH, *J* = 9.4), 8.26–8.29 (d, 2H, ArH, *J* = 8.6), 8.39 (s, 1H, ArH). ^{13}C-NMR (75 MHz, $CDCl_3$): 165.1, 164.6, 163.5, 160.6, 147.8, 146.9, 140.8, 139.1, 134.6, 133.5, 132.7, 130.0, 129.5, 128.7, 127.4, 127.0, 124.4, 122.7, 112.7, 103.7, 101.8, 55.7. ESI-MS: *m/z* 554 ($M+H^+$).

4-(1-(2,4-Dichlorophenyl)-3-(4-nitrophenyl)-1H-pyrazol-4-yl)-6-(4-fluorophenyl)pyrimidin-2-amine (**7l**)

Yield 70%; m.p. 220°C; FT-IR (KBr) ν/cm^{-1}: 3,429 (NH_2), 1,604 (C=C aromatic), 1,344 (NO_2), 1,228 (C–F). ^{1}H-NMR (300 MHz, $CHCl_3$) δ (ppm): 5.75 (s, 2H, NH_2) (D_2O exchangeable), 6.95 (s, 1H, ArH), 7.03–7.06 (d, 2H, ArH, *J* = 9.2), 7.55–7.62 (m, 3H, ArH), 7.83–7.91 (m, 4H, ArH), 8.15–8.18 (d, 2H, ArH, *J* = 9.3), 8.42 (s, 1H, ArH). ^{13}C-NMR (75 MHz, $CDCl_3$): 165.3, 163.1, 161.5, 160.0, 148.8, 146.7, 137.1, 138.9, 136.2, 131.2, 131.8, 130.5, 129.4, 127.5, 123.1, 117.6, 103.7, 101.5. ESI-MS: *m/z* 521 ($M+H^+$).

4-(1-(2,4-Dichlorophenyl)-3-(4-nitrophenyl)-1H-pyrazol-4-yl)-6-(3,4-dimethoxyphenyl)pyrimidin-2-amine (**7m**)

Yield 78%; m.p. 140°C; FT-IR (KBr) ν/cm^{-1}: 3,414 (NH_2), 2,725 (CH aliphatic), 1,602 (C=C aromatic), 1,338 (NO_2). ^{1}H-NMR (300 MHz, $CHCl_3$) δ (ppm): 3.92 (s, 3H, OCH_3), 3.93 (s, 3H, OCH_3), 5.28 (s, 2H, NH_2) (D_2O exchangeable), 6.86 (s, 1H, ArH), 6.89–6.92 (d, 1H, ArH, *J* = 9.2), 7.29–7.33 (dd, 1H, ArH), 7.41–7.45 (dd, 1H, ArH), 7.49 (s, 1H, ArH), 7.60–7.70 (m, 2H, ArH), 7.90–7.93 (d, 2H, ArH), 8.30–8.32 (d, 2H, ArH, *J* = 4.6), 8.41 (s, 1H, ArH). ^{13}C-NMR (75 MHz, $CDCl_3$): 165.4, 163.5, 162.7, 149.2, 149.6, 147.5, 145.1, 141.6, 139.6, 134.6, 134.1, 131.5, 130.0, 129.7, 129.3, 126.1, 123.4, 121.6, 120.9, 111.6, 109.3, 102.9, 100.6, 56.6. ESI-MS: *m/z* 562 ($M+H^+$).

4-(1-(2,4-Dichlorophenyl)-3-(4-nitrophenyl)-1H-pyrazol-4-yl)-6-(2,4-dimethoxyphenyl)pyrimidin-2-amine (**7n**)

Yield 70%; m.p. 180°C; FT-IR (KBr) ν/cm^{-1}: 3,433 (NH_2), 2,723 (CH aliphatic), 1,579 (C=C aromatic), 1,348 (NO_2). ^{1}H-NMR (300 MHz, $CHCl_3$) δ (ppm): 3.53 (s, 3H, OCH_3), 3.74 (s, 3H, OCH_3), 5.39 (s, 2H, NH_2) (D_2O exchangeable), 6.36 (s, 1H, ArH), 6.45–6.47 (d, 1H, ArH), 7.36–7.39 (d, 1H, ArH), 7.50–7.61 (m, 3H, ArH), 7.87–7.90 (d, 3H, ArH, *J* = 9.4), 8.15–8.17 (d, 2H, ArH, *J* = 7.3), 8.35 (s, 1H, ArH). ^{13}C-NMR (75 MHz, $CDCl_3$): 165.2, 163.6, 162.0, 161.6, 158.3, 147.9, 145.8, 141.7, 139.1, 134.9, 133.2, 132.5, 131.6, 131.0, 128.5, 126.1, 123.5, 121.8, 110.2, 103.5, 101.3, 98.8, 56.7, 55.8. ESI-MS: *m/z* 562 ($M+H^+$).

4-(4-Bromophenyl)-6-(1-(2,4-dichlorophenyl)-3-(4-nitrophenyl)-1H-pyrazol-4-yl)pyrimidin-2-amine (**7o**)

Yield 68%; m.p. 240°C; FT-IR (KBr) ν/cm^{-1}: 3,416 (NH_2), 1,602 (C=C aromatic), 1,342 (NO_2), 561 (C–Br). ^{1}H-NMR (300 MHz, $CHCl_3$) δ (ppm): 5.10 (s, 2H, NH_2) (D_2O exchangeable), 6.97 (s, 1H, ArH), 7.41–7.45 (dd, 1H, ArH), 7.55–7.66 (m, 4H, ArH), 7.72–7.75 (d, 2H, ArH, *J* = 8.4), 7.89–7.91 (d, 2H, ArH, *J* = 9.2), 8.26–8.29 (d, 2H, ArH), 8.40 (s, 1H, ArH). ^{13}C-NMR (75 MHz, $CDCl_3$): 165.7, 164.8, 161.5, 148.9, 145.6, 140.7, 139.5, 134.6, 132.5, 131.2, 129.1, 123.7, 123.6, 103.7, 101.6. ESI-MS: *m/z* 604 ($M+Na^+$).

4-(1-(4-Chlorophenyl)-3-(4-nitrophenyl)-1H-pyrazol-4-yl)-6-(4-methoxyphenyl)pyrimidin-2-amine (**7p**)

Yield 80%; m.p. 230°C; FT-IR (KBr) ν/cm^{-1}: 3,441 (NH_2), 2,796 (CH aliphatic), 1,629 (C=C aromatic), 1,332 (NO_2). ^{1}H-NMR (300 MHz, $CHCl_3$) δ (ppm): 3.89 (s, 3H, OCH_3), 5.18 (s, 2H, NH_2) (D_2O exchangeable), 6.86–6.91 (m, 3H, ArH), 7.29–7.32 (d, 2H, ArH, *J* = 7.8), 7.48–7.52 (m, 2H, ArH), 7.75–7.78 (d, 2H, ArH, *J* = 8.2), 7.92–7.94 (d, 2H, ArH, *J* = 6.2), 8.28–8.30 (d, 2H, ArH, *J* = 6.5), 8.48 (s, 1H, ArH). ^{13}C-NMR (75 MHz, $CDCl_3$): 165.0, 163.5, 162.7, 160.8, 147.5, 145.6, 139.6, 137.6, 134.7, 132.6, 130.5, 129.5, 128.6, 128.1, 126.5, 118.6, 115.6, 107.9, 101.6, 55.4. ESI-MS: *m/z* 520 ($M+Na^+$).

4-(1-(4-Chlorophenyl)-3-(4-nitrophenyl)-1H-pyrazol-4-yl)-6-(4-fluorophenyl)pyrimidin-2-amine (**7q**)

Yield 65%; m.p. 280°C; FT-IR (KBr) ν/cm^{-1}: 3,448 (NH_2), 1,597 (C=C aromatic), 1,334 (NO_2), 1,228 (C–F). ^{1}H-NMR (300 MHz, $CHCl_3$) δ (ppm): 5.71 (s, 2H, NH_2) (D_2O exchangeable), 7.05–7.07 (d, 2H, ArH), 7.39–7.42 (d, 2H, ArH, *J* = 8.7), 7.79–7.82 (d, 2H, ArH, *J* = 8.7), 7.87–7.96 (m, 5H, ArH), 8.16–8.19 (d, 2H, ArH, *J* = 8.7), 8.73 (s, 1H, ArH). ^{13}C-NMR (75 MHz, $CDCl_3$): 165.6, 163.4, 161.4, 160.4, 146.7, 145.5, 135.6, 131.5, 131.2, 131.0, 129.7, 128.5, 124.6, 119.6, 116.7, 103.7, 101.7. ESI-MS: *m/z* 508 ($M+Na^+$).

4-(1-(4-Chlorophenyl)-3-(4-nitrophenyl)-1H-pyrazol-4-yl)-6-(3,4-dimethoxyphenyl)pyrimidin-2-amine (**7r**)

Yield 72%; m.p. 230°C; FT-IR (KBr) ν/cm^{-1}: 3,444 (NH_2), 2,725 (CH aliphatic), 1,631 (C=C aromatic), 1,332 (NO_2). ^{1}H-NMR (300 MHz, $CHCl_3$) δ (ppm): 3.91 (s, 3H, OCH_3), 3.92 (s, 3H, OCH_3), 5.17 (s, 2H, NH_2) (D_2O exchangeable), 6.86–6.89 (d, 1H, ArH, *J* = 8.4), 6.92 (s, 1H, ArH), 7.29–7.32 (dd, 1H, ArH), 7.47–7.50 (d, 3H, ArH, *J* = 8.8), 7.76–7.79 (d, 2H, ArH, *J* = 9), 7.92–7.95 (d, 2H, ArH, *J* = 8.7), 8.28–8.31 (d, 2H, ArH, *J* = 9.2), 8.49 (s, 1H, ArH). ^{13}C-NMR (75 MHz, $CDCl_3$): 165.7, 164.7, 161.6, 150.8, 149.6, 147.6, 145.6, 139.7, 135.6,

131.9, 131.6, 130.7, 129.2, 124.5, 120.6, 119.7, 110.0, 107.4, 103.9, 56.1. ESI-MS: *m/z* 529 ($M+Na^+$).

4-(1-(4-Chlorophenyl)-3-(4-nitrophenyl)-1H-pyrazol-4-yl)-6-(2,4-dimethoxyphenyl)pyrimidin-2-amine (**7s**)

Yield 81%; m.p. 210°C; FT-IR (KBr) ν/cm^{-1}: 3,441 (NH_2), 2,748 (CH aliphatic), 1,610 (C=C aromatic), 1,350 (NO_2). ^{1}H-NMR (300 MHz, $CHCl_3$) δ (ppm): 3.58 (s, 3H, OCH_3), 3.84 (s, 3H, OCH_3), 5.04 (s, 2H, NH_2) (D_2O exchangeable), 6.43 (d, 1H, ArH), 6.57–6.60 (dd, 1H, ArH,), 7.23 (s, 1H, ArH), 7.46–7.49 (d, 2H, ArH, *J* = 8.7), 7.75–7.77 (d, 2H, ArH, *J* = 8.7), 7.92–7.97 (m, 3H, ArH), 8.26–8.29 (d, 2H, ArH, *J* = 8.7), 8.43 (s, 1H, ArH). ^{13}C-NMR (75 MHz, $CDCl_3$): 164.1, 163.6, 162.1, 159.3, 158.8, 149.3, 147.6, 139.9, 137.8, 132.9, 131.8, 129.8, 129.7, 129.1, 123.5, 122.6, 120.4, 119.0, 110.3, 105.3, 101.3, 98.7, 55.2, 55.4. ESI-MS: *m/z* 529 ($M+Na^+$).

4-(4-Bromophenyl)-6-(1-(4-chlorophenyl)-3-(4-nitrophenyl)-1H-pyrazol-4-yl)pyrimidin-2-amine (**7t**)

Yield 71%; m.p. 290°C; FT-IR (KBr) ν/cm^{-1}: 3,435 (NH_2), 1,599 (C=C aromatic), 1,344 (NO_2), 567 (C–Br). ^{1}H-NMR (300 MHz, $CHCl_3$) δ (ppm): 5.78 (s, 2H, NH_2) (D_2O exchangeable), 7.08 (s, 1H, ArH), 7.40–7.59 (m, 4H, ArH), 7.64 (s, 1H, ArH), 7.75–7.90 (m, 2H, ArH), 7.93 (d, 2H, ArH, *J* = 9.3), 8.16–8.19 (d, 2H, ArH, *J* = 8.7), 8.25–8.28 (d, 1H, ArH), 8.76 (s, 1H, ArH). ^{13}C-NMR (75 MHz, $CDCl_3$): 165.5, 163.3, 162.1, 147.8, 145.5, 132.6, 131.9, 131.2, 129.5, 128.9, 128.7, 124.2, 123.7, 120.7, 103.8, 101.5. ESI-MS: *m/z* 548 ($M+Na^+$).

4.2 | In vitro anticancer activity

4.2.1 | 3-(4,5-Dimethylthiazol-2-yl)-2,5-diphenyltetrazolium bromide assay

Human breast carcinoma MDA-MB-231 and MCF-7, colon carcinoma HCT116 were cultured in RPMI medium. All the cell cultures were augmented with 2 μM glutamine, 10% fetal bovine serum, 100 units per ml penicillin, and 100 μg/ml streptomycin and incubated at 37°C under 5% CO_2. In vitro cell growth inhibition was assessed with the MTT assay. Cells were seeded into 24-well culture plates at a density of 3,700 cells per ml for MCF-7, 4,000 cells per ml for MDA-MB-231, 3,500 cells per ml for HCT116 and incubated for 24 hr. Then, the cells were incubated with various concentrations of synthesized compounds (**7a–t**) along with standard drug (17-AAG) for 48 hr. The media was removed and MTT reagent (5 mg/10 ml) was added and incubated for 4 hr. Further, the obtained formazan was solubilized by lysis buffer (10% SDS in 0.1 N HCl), DMSO (100 μl/cell), and absorbance was recorded at 570 nm with multi detection reader Spectramax M4, Molecular Devices USA. Control wells contained the equivalent volume of vehicle DMSO (1%). The values shown are the means and standard deviation of at least three independent experiments performed in duplicate.[22,23]

4.2.2 | Fluorescence polarization assay

The ability of test compounds to compete for N-terminal ATP binding site with FITC-labeled geldanamycin determines the potency of compounds to inhibit HSP90α. The N-terminal domain assay kit was procured from BPS Biosciences, San Diego, CA (#50293) and the assay protocol was followed accordingly.[24] The master mixture was prepared with: N wells × (15 μl of Hsp90 assay buffer + 5 μl of 40 mM DTT + 5 μl of 2 mg/ml BSA + 40 of μl H_2O). Then, 65 μl of master mixture was added to all wells. A total of 5 μl of diluted FITC-labeled geldanamycin (100 nM) was added to each well labeled "positive control", "negative control", and "test". A total of 10 μl of test compounds (**7a–c**, **7g**, **7h**, **7j**, **7m**, **7o**, **7p–t**) were added to each well labeled "Test". A total of 25 μl of assay buffer was added to the wells labeled "Blank". Reaction was initiated by adding 20 μl of diluted Hsp90α (17 ng/μl), to each well designated "positive control" and "test" and incubated at room temperature for 2–3 hr with slow shaking. FP values were measured at wavelengths of 485 nm (excitation) and 530 nm (emission) using Biotek Synergy H1 hybrid reader. The fraction of tracer bound to Hsp90 was correlated to the mP value and plotted against values of competitor concentrations. The inhibitor concentration at which 50% of bound GM was displaced was obtained by fitting the data. All experimental data were analyzed using SOFTmax Pro 4.3.1 and plotted using Prism 4.0 (GraphOad Software Inc., San Diego, CA).

4.2.3 | Western blot analysis

MCF-7 cells were seeded at a density of 1×10^6 in 100 cm^2 petri plates. After 24 hr culture, the cells were treated with three different concentrations (0.5, 1, and 2 fold of IC_{50}) of compounds 17-AAG, **7q**, **7t**, or with vehicle (DMSO 0.5%), for 24 hr. After completion, cells were trypsinised and washed with phosphate buffered saline and then with lysis solution (50 mM Tris-HCl pH 7.4, 150 mM NaCl, 2 mM ethylenediaminetetraacetic acid, 1% NP-40 (v/v), 0.1% sodium dodecyl sulfate (SDS; w/v), 5 mM dithiothreitol, and protease inhibitor). Lysate protein concentration was determined by the bicinchoninic acid protein assay (Thermo Scientific) and equal amount of protein from each lysate was loaded on SDS polyacrylamide gel electrophoresis and blotted onto polyvinylidene fluoride membrane (Millipore), conjugated with specific primary antibodies and then probed with goat anti-rabbit antibody coupled to peroxidase antibody. The bands were visualized on a chemiluminescence plate reader. Expression of pHER2 and pErk1/2 proteins was determined by probing with specific pHER2 and pERK1/2 antibodies, (#6942 and #9101, Cell Signaling Technology, Danvers, MA). Here, β-actin was taken as loading control.[25]

4.3 | Docking studies

The PDB entry 5LRZ (a co-crystal of A003643501 in complex with HSP90α) was downloaded from Protein Data Bank due to its structural resemblance with test series and were docked at N-terminal ATP binding site HSP90α using Glide program embedded in Maestro 9.1 on Schrodinger engine. The downloaded PDB was further processed for energy minimization and then grid was generated at active site. The ligands were subjected to ligprep

simulations to generate energy minimized 3D structures and were docked flexibly in the protein grids using Glide-extra precision (XP) simulations. The final docking score (g score) was based on interactions such as lipophilic pair term, hydrophobic enclosure reward, hydrogen bonding and electrostatic rewards. The performed docking was validated by superimposing the docked A003643501 with cocrystal ligand and the RMSD was less than 0.01.

ACKNOWLEDGMENTS

This research was supported by Women Scientist Scheme (WOS-A), Department of Science and Technology (DST), New Delhi, India (Grant no. SR/WOS-A/CS-1003/2014).

CONFLICT OF INTEREST

The authors declare that there is no conflict of interest.

ORCID

Naikal James Prameela Subhashini http://orcid.org/0000-0003-3852-6043

REFERENCES

[1] J. H. Bauer, S. L. Helfand, *Aging Cell* **2006**, *5*, 437.
[2] F. U. Hartl, A. Bracher, M. Hayer-Hartl, *Nature* **2011**, *475*, 324.
[3] S. H. David, B. Udai, T. Bahareh, C. G. Goldy, A. Joann, K. Razelle, *Cancer Treat. Rev.* **2012**, *39*, 375.
[4] S. M. Roe, C. Prodromou, R. O'brien, J. E. Ladbury, P. W. Piper, L. H. Pearl, *J. Med. Chem.* **1999**, *42*, 260.
[5] C. E. Stebbins, A. A. Russo, C. Schneider, N. Rosen, F. U. Hartl, N. P. Pavletich, *Cell* **1997**, *89*, 239.
[6] T. Taldone, W. sun, G. Chiosis, *Bioorg. Med. Chem.* **2009**, *17*, 2225
[7] G. Chiosis, B. Lucas, A. Shtil, H. Huezo, N. Rosen, *Bioorg. Med. Chem.* **2002**, *10*, 3555.
[8] P. P. Kung, L. Funk, J. Meng, M. Collins, J. Z. Zhou, M. Catherine johnson, A. Ekker, J. Wang, P. Mehta, M. J. Yin, C. Rodgers, J. F. Davies, E. Bayman, T. Smeal, K. A. Maegley, M. R. Gehring, *Bioorg. Med. Chem. Lett.* **2008**, *18*, 6273.
[9] D. L. Menezes, P. Taverna, M. R. Jensen, T. Abrams, D. Stuart, G. K. Yu, D. Duhl, T. Machajewski, W. R. Sellers, N. K. Pryer, Z. Gao, *Mol. Cancer Ther.* **2012**, *11*, 730.
[10] M. Drysdale, P. Brough, *Curr. Top. Med. Chem.* **2008**, *8*, 859.
[11] A. Suda, H. Koyano, T. Hayase, K. Hada, K. Kawasaki, S. Komiyama, K. Hasegawa, T. A. Fukami, S. Sato, T. Miura, N. Ono, T. Yamazaki, R. Saitoh, N. Shimma, Y. Shiratori, T. Tsukuda, *Bioorg. Med. Chem.* **2012**, *22*, 1136.
[12] T. J. Hong, H. Park, Y. J. Kim, J. H. Jeong, J. S. Hahn, *Bioorg. Med. Chem. Lett.* **2009**, *19*, 4839.
[13] C. Prodromou, L. Pearl, *Curr. Cancer Drug Targets* **2003**, *3*, 301.
[14] M. P. Goetz, D. O. Toft, M. Ames, C. Erlichman, *Ann. Oncol.* **2003**, *14*, 1169.
[15] G. V. Georgakis, Y. Li, G. Z. Rassidakis, H. M. Valdez, L. J. Medeiros, A. Younes, *Clin. Cancer Res.* **2006**, *12*, 584.
[16] J. Shi, R. Van de Water, K. Hong, R. B. Lamer, K. W. Weichert, C. M. Sandoval, S. R. Kasibhatla, M. F. Boehm, J. Chao, K. Lundgren, N. Timple, R. Lough, G. Ibanez, C. Boykin, F. J. Burrows, M. R. Kehry, T. J. Yun, E. K. Harning, C. Ambrose, J. Thompson, S. A. Bixler, A. Dunah, P. Snodgrass-Belt, J. Arndt, I. J. Enyedy, P. Li, V. S. Hong, A. McKenzie, M. A. Biamonte, *J. Med. Chem.* **2012**, *55*, 7786.
[17] W. He, H. Hu, *Oncol. Rep.* **2018**, *40*, 3.
[18] M. A. Kira, M. O. Abdel-Rahman, K. Z. Gadalla, *Tetrahedron Lett.* **1969**, *10*, 109.
[19] B. Insuasty, A. Tigreros, F. Orozco, J. Quiroga, R. Abonía, M. Nogueras, A. Sanchez, J. Cobo, *Bioorg. Med. Chem.* **2010**, *18*, 4965.
[20] S. Sakkiah, S. Thangapandian, S. John, K. W. Lee, *Eur. J. Med. Chem.* **2011**, *46*, 2937.
[21] S. Roughley, L. Wright, P. Brough, A. Massey, R. E. Hubbard, *Top. Curr. Chem.* **2012**, *317*, 61.
[22] J. H. Lee, S. C. Shin, S. H. Seo, Y. H. Seo, N. Jeong, C. W. Kim, E. E. Kim, G. Keum, *Bioorg. Med. Chem. Lett.* **2017**, *27*, 237.
[23] Y. Priyadarshini Devi, A. Uma, M. Lakshmi Narasu, C. Kalyani, *Int. J. Res. Appl. Nat. Soc. Sci.* **2014**, *2*, 269.
[24] J. Kim, S. Felts, L. Lauger, H. He, H. Huezo, N. Rosen, G. Chiosis, *J. Biomol. Screen.* **2004**, *9*, 375.
[25] S. Y. Park, Y. J. Oh, Y. Lho, J. H. Jeong, K. H. Liu, J. Song, S. H. Kim, E. Ha, Y. H. Seo, *Eur. J. Med. Chem.* **2018**, *143*, 390.

SUPPORTING INFORMATION

Additional supporting information may be found online in the Supporting Information section.

How to cite this article: Mettu A, Talla V, Bajaj DM, Prameela Subhashini NJ. Design, synthesis and molecular docking studies of novel pyrazolyl 2-aminopyrimidine derivatives as HSP90 inhibitors. *Arch Pharm Chem Life Sci.* 2019;e1900063. https://doi.org/10.1002/ardp.201900063